Journal of Statistical Physics, Vol. 72, Nos. *1/2, 1993*

Potential Theory and Analytic Properties of Self-Similar Fractal and Multifractal Distributions

C. P. Dettmann[1] and N. E. Frankel[1]

Received December 31, 1992

By the use of recursion relations and analytic techniques we deduce general analytic results pertaining to the electrostatic potential, moments, and Fourier transform of exactly self-similar fractal and multifractal charge distributions. Three specific examples are given: the binomial distribution on the middle-third Cantor set, which is a multifractal distribution, the uniform distribution on the Menger sponge, which illustrates the added complication of higher dimensionality, and the uniform distribution on the von Koch snowflake, which illustrates the effect of rotations in the defining transformations.

KEY WORDS: Multifractal Cantor; Menger and Koch fractals; potential theory; Mellin and Fourier transforms.

1. INTRODUCTION

There are a number of interrelated physical systems which involve Laplace's equation with fractal boundary conditions. These include gravitationally interacting structures such as the distribution of galaxies[1] and Saturn's rings[2]; the electrodynamic processes which generate diffusion-limited aggregates[3]; the eigenmodes of a fractal drum[4]; and diffraction from random[5,6] and deterministic[7,8] fractal objects. The scale invariance of fractals and their diffraction patterns has recently been used to design wide-bandwidth acoustical diffusors.[9]

For the case of the galaxy distribution, as well as that of diffusion-limited aggregation, the distribution of mass (respectively, charge) is not uniform over its fractal support set. Rather, it exhibits different scaling

[1] School of Physics, University of Melbourne, Parkville, Victoria 3052, Australia.

0022-4715/93/0700-0241$07.00/0 © 1993 Plenum Publishing Corporation

exponents at different points on the fractal, and as such is called a multifractal distribution. An introduction to multifractal formalisms is found in Chapter 17 of ref. 10.

One problem that arises in these systems is to calculate the electrostatic potential from a given fractal or multifractal charge distribution. While mathematicians have studied the general structure of the potential about singular points,[11] there has been very little detailed analytical work with application to specific fractals. Bessis *et al.*[12] investigated the Mellin transform and various other analytic properties of Julia sets, fractals generated by a single nonlinear transformation on the complex field. The Mellin transform was found to contain a semi-infinite array of poles. From the residues of these poles, power series expansions for the potential near points on the fractal may be generated, although they did not do this explicitly. These results need to be generalized, since many important fractals are of higher dimension than that of Julia sets (two), and/or require more than one transformation to represent them. Here, we use only similarity transformations, but place no restrictions on the embedding dimension E or the number of transformations N.

In our earlier paper[13] we used Mellin transforms to evaluate a power series expansion for the potential near the end of a uniform distribution of charge on the middle-third Cantor set. It was found that, in addition to the $r^{\ln 2/\ln 3 - 1}$ behavior, there are oscillations in the logarithm of the distance from the fractal, resulting from a vertical infinite sequence of poles in the Mellin transform. In addition, we investigated the asymptotic behavior of the moments of this distribution, finding oscillatory behavior which could be related to the oscillations in the potential.

In Section 2 of this paper we generalize the method to include all self-similar multifractal distributions, a subset of which are the uniform distributions on self-similar fractals. Explicit calculations are then given for the binomial distribution on the Cantor set (Section 3), the uniform distribution on the Menger sponge (Section 4), and the uniform distribution on the von Koch snowflake (Section 5). These specific examples permit the calculations to be carried out to a greater degree than the general case of Section 2, and also allow the effects of the multifractal structure, higher dimensionality, and the presence of rotations in the defining transformations to be investigated separately.

Also included in each section is an analysis of the Fourier transform of the distribution, of much relevance to diffraction problems, but also of interest in its own right. The Fourier transform of the Cantor set has been known for some time.[14] Allain and Cloitre[7] used convolution techniques to extend this to self-similar fractals without rotations, investigating the conditions under which the Fourier transform approaches zero, as $\mathbf{k} \to \infty$.

We extend the treatment to multifractal distributions, and allow for rotations, and make some progress regarding the convergence of the Fourier transform as $\mathbf{k} \to \infty$ for a distribution defined using rotations.

2. GENERAL THEORY

A large class of fractals have the property that they are exactly self-similar, that is, they may be split into N parts, each of which is a contracted, rotated, and/or reflected version of the original. For a fractal set $\mathbf{F}$ this is written

$$\mathbf{F} = \bigcup_{\alpha=1}^{N} \mathbf{F}_\alpha \tag{2.1}$$

$$\mathbf{F}_\alpha = S_\alpha \mathbf{F} \tag{2.2}$$

The similarity transformation S_α may be written as the combination of an isotropic dilation factor $0 < c_\alpha < 1$, a unitary rotation/reflection matrix U_α, and a translation by a constant vector $\mathbf{t}_\alpha$, all in an E-dimensional Euclidean space $\mathbf{R}^E$. It is sometimes convenient to treat the linear part of the transformation, denoted by L_α, separately:

$$S_\alpha \mathbf{x} = c_\alpha U_\alpha \mathbf{x} + \mathbf{t}_\alpha = L_\alpha \mathbf{x} + \mathbf{t}_\alpha \tag{2.3}$$

There are several definitions of the dimension of a fractal. For a self-similar fractal with the $\mathbf{F}_\alpha$ nonoverlapping, the Hausdorff and box-counting dimensions[10] are both given by the solution of

$$\sum_{\alpha=1}^{N} c_\alpha^{\dim} = 1 \tag{2.4}$$

For the case of uniform distributions (defined below), this value appears repeatedly throughout the calculations. On the other hand, if the distribution is multifractal (see Section 3) there are several effective dimensions, depending on the quantity to be measured, the point on the fractal, and so on.

On our fractal set $\mathbf{F}$ we now place a charge distribution $\rho(\mathbf{x})$. Like the Dirac distribution, this is singular at points of $\mathbf{F}$ and zero elsewhere; however, integrals of $\rho(\mathbf{x})$ over any region are finite. The self-similarity of the fractal appears in the definition of $\rho(\mathbf{x})$ in a natural way:

$$\rho(\mathbf{x}) = \sum_{\alpha=1}^{N} \lambda_\alpha \rho(\mathbf{S}_\alpha^{-1}\mathbf{x}) \tag{2.5}$$

with normalization

$$\int_{-\infty}^{\infty} \rho(\mathbf{x})\, d^E x = 1 \tag{2.6}$$

The weighting factors λ_α determine the total charge on each of the subsets $\mathbf{F}_\alpha$. For the distributions considered here the λ_α are constant, although generally they are functions of $\mathbf{x}$. In this case the normalization condition above is equivalent to

$$\sum_{\alpha=1}^{N} \lambda_\alpha c_\alpha^E = 1 \tag{2.7}$$

A uniform distribution, where identical regions of the fractal have the same charge, is characterized by

$$\lambda_\alpha = \frac{c_\alpha^{-E}}{N} \tag{2.8}$$

The electrostatic potential around the fractal in $\beta+2$ dimensions is given as

$$V_\beta(\mathbf{x}) = \int_{-\infty}^{\infty} \frac{\rho(\mathbf{x}')\, d^E x'}{|\mathbf{x}-\mathbf{x}'|^\beta}, \qquad \beta \neq 0 \tag{2.9}$$

Note that although the integration is carried over E dimensions, $\mathbf{x}$ is an element of a higher $(\beta+2)$-dimensional space. The recursion relation (2.5) gives

$$V_\beta(\mathbf{x}) = \sum_{\alpha=1}^{N} \lambda_\alpha c_\alpha^{E-\beta} V_\beta(S_\alpha^{-1}\mathbf{x}) \tag{2.10}$$

If $\beta=0$ (two-dimensional space), the appropriate expression for the potential is

$$V_0(\mathbf{x}) = -\int_{-\infty}^{\infty} \rho(\mathbf{x}') \ln |\mathbf{x}-\mathbf{x}'|\, d^E x' \tag{2.11}$$

which readily yields the recursion relation

$$V_0(\mathbf{x}) = \sum_{\alpha=1}^{N} \lambda_\alpha c_\alpha^E (V_0(S_\alpha^{-1}\mathbf{x}) - \ln c_\alpha) \tag{2.12}$$

The Fourier transform of the distribution is defined by

$$\tilde{\rho}(\mathbf{k}) = \int_{-\infty}^{\infty} \rho(\mathbf{x})\, e^{i\mathbf{k}\cdot\mathbf{x}}\, d^E x \tag{2.13}$$

Using Eq. (2.5) gives

$$\tilde{\rho}(\mathbf{k}) = \sum_{\alpha=1}^{N} \lambda_\alpha c_\alpha^E e^{i\mathbf{k}\cdot t_\alpha} \tilde{\rho}(L_\alpha^\dagger \mathbf{k}) \tag{2.14}$$

where the dagger indicates Hermitian conjugate, and is simply the transpose of L_α, since the L_α are real matrices. If all of the L_α are the same, as for the Cantor set and Menger sponge, the above, the above recursion relation may be iterated to give an infinite product representation for $\tilde{\rho}(\mathbf{k})$,

$$\tilde{\rho}(\mathbf{k}) = \prod_{j=0}^{\infty} \left[\sum_{\alpha=1}^{N} \lambda_\alpha c_\alpha^E \exp(iL^{\dagger j}\mathbf{k}\cdot\mathbf{t}_\alpha) \right] \tag{2.15}$$

The moments of the distribution are defined in the usual way,

$$\rho_{\{a_j\}} = \int_{-\infty}^{\infty} \rho(\mathbf{x}) \left(\prod_{j=1}^{E} x_j^{a_j} \right) d^E x \tag{2.16}$$

Substituting this into the recursion relation (2.5) gives a recursion relation for the moments, which are usually better to calculate individually for each $\rho(\mathbf{x})$. If the S_α contain no rotations, as in Sections 3 and 4, the $\rho_{\{a_j\}}$ can be calculated iteratively, beginning with small of the a_j. The presence of rotations "mixes" the equations, so that the $\rho_{\{a_j\}}$ with $\sum_{j=1}^{E} a_j = n$ are determined in terms of each other, as well as lower values of the a_j. This is illustrated by the Koch snowflake in Section 5.

Expanding the exponential in Eq. (2.13) in a Taylor series gives an expression for the moments in terms of the Fourier transform,

$$\rho_{\{a_j\}} = (-i)^{\sum_{j=1}^{E} a_j} \prod_{j=1}^{E} \left(\frac{\partial}{\partial k_j} \right)^{a_j} \tilde{\rho}(\mathbf{k}) \bigg|_{\mathbf{k}=0} \tag{2.17}$$

Expanding the integrand of Eq. (2.9) or Eq. (2.11) in a Taylor series gives an expansion for the potential which converges far from the fractal, in terms of the moments. At points close to the fractal the recursion relations (2.10), (2.12) may be used to find the potential in terms of itself evaluated at points at which the expansion is convergent.

This concludes the general remarks about self-similar fractals. The rest of this paper consists of specific examples, where the deeper structure of the above expressions is more evident, and the effects of various properties of the distributions may be examined separately.

3. BINOMIAL CANTOR DISTRIBUTION

3.1. Definition

The "middle-third Cantor set" is defined by an iterative process. Start with a line segment, which we specify as $(-1/2, 1/2)$ on the x-axis. Remove the middle third, to leave two segments, each one-third of the original length. Repeat this process with each of the two segments obtained, and so on. The result is shown on the bottom line of Fig. 1.

The Cantor set is self-similar in the sense defined in Section 2, that is, it is equivalent to two reduced copies of itself, with the transformations defined as

$$S_1(x) = \frac{x-1}{3} \tag{3.1}$$

$$S_2(x) = \frac{x+1}{3} \tag{3.2}$$

The binomial distribution on the Cantor set is the distribution for which (a) both copies of the set have charge distributions which are scaled-down versions of the whole, and (b) the right half of the set has total charge p, while the left half has $1-p$. This distribution $C_p(x)$ is depicted schematically in Fig. 2 for the case $p = 2/3$. The recursion relation for $C_p(x)$, which can easily be obtained from Eqs. (2.5), 2.7), is

$$C_p(x) = 3[(1-p)\, C_p(3x+1) + pC_p(3x-1)] \tag{3.3}$$

The restriction $p \geqslant 1/2$ may be made without loss of generality, since replacing p by $1-p$ simply reflects the distribution across $x = 0$.

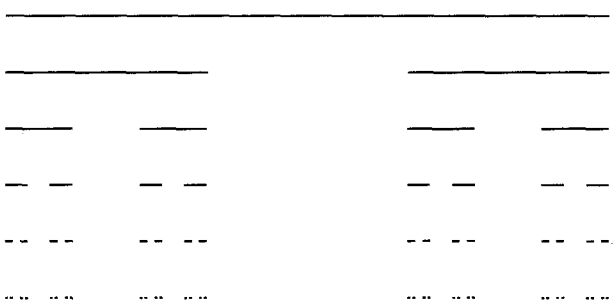

Fig. 1. The construction of the Cantor set. The ends of the line segment shown are taken to have coordinates $(-1/2, 0)$ and $(1/2, 0)$.

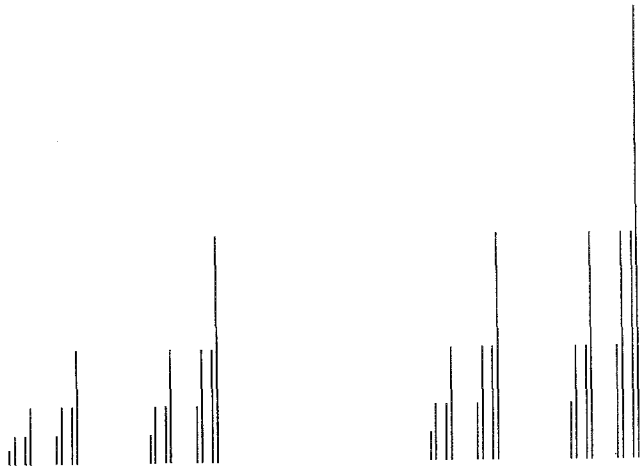

Fig. 2. A representation of the binomial distribution on the Cantor set, for $p = 2/3$. The length of each line is proportional to the amount of charge on part of the Cantor set.

In the case $p = 1/2$, $C_p(x)$ reduces to the uniform case treated in our earlier paper[13]; many of the results of that paper are obtained as a special case of the results presented here. If p is equal to 1 (or 0), the distribution is concentrated at 1/2 (respectively, $-1/2$) and reduces to a shifted Dirac distribution.

For other values of p the distribution is multifractal, meaning that effective dimensions (there are several possible definitions) differ from point to point on the fractal. This is shown explicitly here for the effective dimension defined using the power law of the potential. Chapter 17 of ref. 10 gives an introductory explanation of multifractals, with the binomial Cantor distribution as the main example. It also defines the multifractal spectrum $f(\alpha)$, which is an important aspect of this subject, but not one we will have need of in our calculations.

3.2. Potential

The electrostatic potential from the binomial Cantor distribution in three dimensions is given by Eq. (2.9),

$$V_p(x, y) = \int_{-\infty}^{\infty} \frac{C_p(x')\, dx'}{[(x-x')^2 + y^2]^{1/2}} \tag{3.4}$$

The generalization of this to nonzero values of z is trivial. Expanding the integrand in a Taylor series about $x'=0$ gives an expression which converges for large x and/or y,

$$V_p(x, y) = \sum_{n=0}^{\infty} \frac{C_{p;n}}{n!} \frac{\partial^n}{\partial x'^n} \frac{1}{[(x-x')^2+y^2]^{1/2}}\bigg|_{x'=0} \tag{3.5}$$

Here, $C_{p;n}$ are the moments of the distribution, defined by

$$C_{p;n} = \int_{-\infty}^{\infty} C_p(x)\, x^n\, dx \tag{3.6}$$

These are evaluated and discussed in the next subsection.

V_p also satisfies the recursion relation (2.10),

$$V_p(x, y) = 3pV_p(3x-1, 3y) + 3(1-p)\, V_p(3x+1, 3y) \tag{3.7}$$

We will not do a complete analysis of the potential here; we are most interested in its behavior near the fractal, and in particular how the dimensionality of the distribution appears in the form of power laws. First we consider the potential along the line $x=1/2$, for small y. This corresponds to a line coming vertically down to the right-hand endpoint of the fractal. Equation (3.7) gives

$$V_p(1/2, y) = 3pV_p(1/2, 3y) + 3(1-p)\, V_p(5/2, 3y) \tag{3.8}$$

The first term in this expression corresponds to a point which is still near the fractal, so the recursion relation is used iteratively to obtain

$$V_p\left(\frac{1}{2}, y\right) = \sum_{j=0}^{\infty} \frac{1-p}{p} (3p)^{j+1}\, V_p\left(\frac{5}{2}, 3^{j+1}y\right) \tag{3.9}$$

Note that this series does converge, since the potential approaches zero at large distances. Equation (3.5) is now substituted to obtain

$$V_p\left(\frac{1}{2}, y\right) = \sum_{j=0}^{\infty} \frac{1-p}{p} (3p)^{j+1} \sum_{n=0}^{\infty} \frac{C_{p;n}}{n!} \frac{\partial^n}{\partial x'^n} \times \frac{1}{[(5/2-x')^2+(3^{j+1}y)^2]^{1/2}}\bigg|_{x'=0} \tag{3.10}$$

The power law (or logarithmic) dependence of this expression on y is best obtained using Mellin transform technique.[15] The argument of the derivative is written as the inverse Mellin of its Mellin transform, using y^2

as the Mellin variable. Care must be taken with the sign of the $(5/2-x')$ term. Then the derivative is performed, and also the sum over j, which becomes a geometric series. The result is

$$V_p\left(\frac{1}{2}, y\right)=\frac{1-p}{p}\sum_{n=0}^{\infty}\frac{(-1)^n C_{p;n}}{n!}\frac{1}{2\pi i}$$
$$\times\int_{c-i\infty}^{c+i\infty} ds\,|y|^{-2s}\frac{1}{3^{2s-1}/p-1}$$
$$\times\frac{\Gamma(s)\,\Gamma(1/2-s)}{\Gamma(1/2)}\frac{\Gamma(2s)}{\Gamma(2s-n)}\left(\frac{5}{2}\right)^{2s-n-1} \tag{3.11}$$

where

$$\frac{1}{2}\left(1+\frac{\ln p}{\ln 3}\right)<c<\frac{1}{2} \tag{3.12}$$

Note that the potential is an even value of y, hence the absolute value signs. The integral is evaluated by closing the contour to the left and using Cauchy's theorem. The leading term (smallest power of $|y|$) comes from the denominator, which has a line of poles of residue $1/(2\ln 3)$ at

$$s=s_m\equiv\frac{1}{2}\left(1+\frac{\ln p}{\ln 3}+\frac{2\pi i m}{\ln 3}\right) \tag{3.13}$$

In addition, the gamma function $\Gamma(z)$ has a pole of residue $(-1)^q/q!$ at $z=-q$ for all nonnegative integers q. This gives a power series in even powers of y. The result is

$$V_p\left(\frac{1}{2}, y\right)=\frac{1-p}{2p\ln 3}\sum_{n=0}^{\infty}\sum_{m=-\infty}^{\infty}\frac{(-1)^n C_{p;n}}{n!}|y|^{-2s_m}$$
$$\times\frac{\Gamma(s_m)\,\Gamma(1/2-s_m)\,\Gamma(2s_m)}{\Gamma(1/2)\,\Gamma(2s_m-n)}\left(\frac{5}{2}\right)^{2s_m-n-1}$$
$$+\frac{1-p}{p}\sum_{n=0}^{\infty}\sum_{q=0}^{\infty}\frac{(-1)^q\,(2q+n)!\,C_{p;n}}{q!\,(2q)!\,n!}$$
$$\times\frac{|y|^{2q}}{3^{-2q-1}/p-1}\frac{\Gamma(q+1/2)}{\Gamma(1/2)}\left(\frac{5}{2}\right)^{-2q-n-1} \tag{3.14}$$

The first series gives a power law corresponding to a dimension of $-\ln p/\ln 3$, which reduces to the dimension of the fractal in the case of a uniform distribution ($p=1/2$). Since the point at $x=1/2$ has the greatest

charge "density," this corresponds to the largest dimension associated with this multifractal distribution. The terms corresponding to nonzero m result in oscillations in the logarithm of $|y|$, as for the uniform case.[13] The coefficients of these terms decrease exponentially with $|m|$, due to the gamma functions of complex argument. It can be shown using the results of the next section that the second series converges for $|y| \leqslant 2$ for all $0 < p < 1$.

If the contour is closed to the right, the large-y expansion is obtained. The result, which agrees with a more direct evaluation of Eq. (3.5), is

$$\begin{aligned} V_p\left(\frac{1}{2}, y\right) &= \sum_{q=0}^{\infty} |y|^{-1-2q} \sum_{n=0}^{\infty} \frac{(-1)^{n+q}\,(2q)!\, C_{p;n}}{q!\, n!\, (2q-n)!} \frac{\Gamma(q+1/2)}{\Gamma(1/2)} \\ &\quad \times \left(\frac{5}{2}\right)^{2q-n} \frac{1-p}{3^{2q}-p} \\ &= \frac{1}{|y|} - \frac{p^2-3p+2}{4\,|y|^3} \\ &\quad + \frac{9p^4-198p^3+993p^2-1584p+780}{2080\,|y|^5} + \cdots \end{aligned} \tag{3.15}$$

The potential near the opposite end of the fractal, at $(-1/2, y)$, may be obtained by replacing p by $1-p$ in the above analysis. The result is an effective dimension of $-\ln(1-p)/\ln 3$ at this point, which is thus the smallest effective dimension of this distribution.

The other point we consider is $x = 1/4$. This is the point obtained by choosing first the right segment of the fractal, then the left subsegment, then the right subsubsegment, ad infinitum. The recursion relation (3.7) gives

$$\begin{aligned} V_p\left(\frac{1}{4}, y\right) &= 3pV_p\left(-\frac{1}{4}, 3y\right) + 3(1-p)\, V_p\left(\frac{7}{4}, 3y\right) \\ &= 3p\left[3pV_p\left(-\frac{7}{4}, 9y\right) + 3(1-p)\, V_p\left(\frac{1}{4}, 9y\right)\right] \\ &\quad + 3(1-p)\, V_p\left(\frac{7}{4}, 3y\right) \\ &= \sum_{j=0}^{\infty} [9p(1-p)]^{j+1} \left[\frac{1}{3p} V_p\left(\frac{7}{4}, 3^{2j+1}y\right)\right. \\ &\quad \left. + \frac{p}{1-p} V_p\left(-\frac{7}{4}, 3^{2j+2}y\right)\right] \end{aligned} \tag{3.16}$$

This expression is manipulated in exactly the same manner as Eq. (3.9) to obtain

$$V_p\left(\frac{1}{4}, y\right) = \frac{1}{4\ln 3} \sum_{n=0}^{\infty} \sum_{m=-\infty}^{\infty} \frac{C_{p;n}}{n!} |y|^{-2s_m} \frac{\Gamma(s_m)\,\Gamma(1/2 - s_m)\,\Gamma(2s_m)}{\Gamma(1/2)\,\Gamma(2s_m - n)}$$
$$\times \left(\frac{7}{4}\right)^{2s_m - n - 1} [3^{2s_m} + (-1)^n]$$
$$+ \sum_{n=0}^{\infty} \sum_{q=0}^{\infty} \frac{(-1)^{q+n}\,(2q+n)!\,C_{p;n}}{q!\,(2q)!\,n!}$$
$$\times \frac{|y|^{2q}}{3^{-4q-2}/p(1-p) - 1} \frac{\Gamma(q+1/2)}{\Gamma(1/2)}$$
$$\times \left(\frac{7}{4}\right)^{-2q-n-1} [3^{-2q} + (-1)^n] \tag{3.17}$$

$$s_m = \frac{1}{2}\left(1 + \frac{\ln p(1-p)}{2\ln 3} + \frac{2\pi i m}{2\ln 3}\right) \tag{3.18}$$

Thus the effective dimension at this point out to $\ln p(1-p)/(2\ln 3)$, which is just the arithmetic mean of that of the two endpoints. The second series converges for $|y| \leqslant 5/4$. This procedure generalizes to any rational point on the Cantor set, that is, any point which is transformed to points which are mapped onto themselves after a finite number of transformations.

It is also possible to calculate the potential near the ends of the fractal, but along the x axis. The recursion relation (3.7) gives

$$V_p\left(x + \frac{1}{2}, 0\right) = 3pV_p\left(3x + \frac{1}{2}, 0\right) + 3(1-p)\,V_p\left(3x + \frac{5}{2}, 0\right)$$
$$= \frac{1-p}{p} \sum_{j=0}^{\infty} (3p)^{j+1}\,V_p\left(3^{j+1}x + \frac{5}{2}, 0\right) \tag{3.19}$$

Substituting Eq. (3.5) and performing the multiple derivative gives

$$V_p\left(x + \frac{1}{2}, 0\right) = \frac{1-p}{p} \sum_{j=0}^{\infty} (3p)^{j+1} \sum_{n=0}^{\infty} \frac{C_{p;n}}{(3^{j+1}x + 5/2)^{n+1}} \tag{3.20}$$

which is then Mellin transformed with respect to x, and the contour integral performed by closing to the left to obtain the small-x expansion,

$$V_p\left(x+\frac{1}{2},0\right)=\frac{1}{\ln 3}\frac{1-p}{p}\sum_{n=0}^{\infty}\frac{C_{p;n}}{n!}\sum_{m=-\infty}^{\infty}\Gamma(s_m)$$
$$\times\Gamma(n+1-s_m)\left(\frac{2}{5}\right)^{n+1-s_m}x^{-s_m}$$
$$+\frac{1-p}{p}\sum_{n=0}^{\infty}C_{p;n}\sum_{q=0}^{\infty}\frac{(-1)^q(n+q)!}{n!\,q!}$$
$$\times\left(\frac{2}{5}\right)^{n+q+1}\frac{x^q}{3^{-q-1}/p-1} \tag{3.21}$$

$$s_m=1+\frac{\ln p}{\ln 3}+\frac{2\pi i m}{\ln 3} \tag{3.22}$$

Note that the effective dimension $-\ln p/\ln 3$ is the same as the previous case [Eq. (3.14)], as is the constant term (coefficient of x^0). The second series converges for $x\leqslant 2$. Closing the contour to the right generates the large-x expansion,

$$V_p\left(x+\frac{1}{2},0\right)=\sum_{q=0}^{\infty}x^{-1-q}\sum_{n=0}^{q}\left(-\frac{5}{2}\right)^{q-n}\frac{q!}{n!\,(q-n)!}\frac{1-p}{3^q-p}$$
$$=\frac{1}{x}-\frac{1-p}{x^2}+\frac{2-3p+p^2}{2x^3}-\frac{26-47p+24p^2-3p^3}{26x^4}$$
$$+\frac{260-528p+331p^2-66p^3+3p^4}{260x^5}+\cdots \tag{3.23}$$

3.3. Moments

Now we consider the moments of the distribution, the $C_{p;n}$ defined by Eq. (3.6). Substituting the recursion relation (3.3) into this definition and using the binomial theorem yields a recursion relation for the moments:

$$C_{p;n}=\frac{1}{3^n-1}\sum_{j=0}^{n-1}C_{p;j}\binom{n}{j}[p+(1-p)(-1)^{n-j}] \tag{3.24}$$

The $C_{p;n}$ are polynomials in p with rational coefficients. The first few are tabulated in Table I. They rapidly become more complicated, and it is difficult to see what the behavior is as $n\to\infty$. Unlike the uniform case, there are now both even and odd moments, and it is interesting to consider the limit $p\to 1/2$, where all the odd moments vanish. In general,

$$C_{1-p;n}=(-1)^n C_{p;n} \tag{3.25}$$

Table I. Moments of the Binomial Cantor Distribution

n	$C_{p;n}$
0	1
1	$(2p-1)/2$
2	$(2p^2-2p+1)/4$
3	$(12p^3-18p^2+32p-13)/104$
4	$(12p^4-24p^3+184p^2-172p+65)/1040$
5	$(24p^5-60p^4+2712p^3-4008p^2+4478p-1573)/50336$
6	$(72p^6-216p^5+68484p^4-136608p^3+496670p^2-428402p+143143)/9161152$

We now proceed to find the large-n limit of the $C_{p;n}$, beginning with the ansatz

$$C_{p;n}=a^n[F(n)+(-1)^n\,G(n)] \tag{3.26}$$

This ansatz is a natural extension of the $p=1/2$ result.[13] The F and G functions are assumed to be "slowly varying,"

$$\frac{F'(n)}{F(n)},\ \frac{G'(n)}{G(n)} \ll n^{-1/2} \tag{3.27}$$

At all times during this calculation we omit terms which are a factor $1/n$ smaller than the dominant terms. Thus Stirling's formula, which is used to simplify the binomial coefficient, is written

$$q!=q^q e^{-q}(2\pi q)^{1/2}\,[1+O(1/q)] \tag{3.28}$$

Note that since the contribution of the endpoints of the sum in Eq. (3.24) is negligible due to the binomial coefficient, irrespective of the value of a, both j and $n-j$ are of order n, so the use of Stirling's formula for their factorials is valid. Thus the summand of Eq. (3.24) may be written

$$\left[\frac{a^y}{y^y(1-y)^{1-y}}\right]^n \frac{n^{-1/2}}{[2\pi y(1-y)]^{1/2}}\,[pF(yn) + (-1)^n\,(1-p)\,G(yn)] \tag{3.29}$$

where

$$j=yn \tag{3.30}$$

Here, the alternating sign given by $(-1)^j$ has already been averaged over. The terms which contribute to the sum are around

$$y_{\max} = \frac{a}{1+a} \tag{3.31}$$

and are of order $\sqrt{n}$ in number; thus all terms which do not have n as the exponent are effectively constant over this range. The sum is written as an integral, with the Euler–Maclaurin corrections being of order $1/n$. The result is

$$C_{p;n} = \frac{1}{3^n} \frac{n^{-1/2}}{[2\pi y_{\max}(1-y_{\max})]^{1/2}} [pF(yn) + (-1)^n (1-p)\, G(yn)] \times \int_0^1 n\, dy \left[\frac{a^y}{y^y(1-y)^{1-y}}\right]^n \tag{3.32}$$

The integral is evaluated using the method of steepest descents; that is, the integrand is written as an exponential, the argument of which is expanded in a Taylor series about its maximum, to give

$$\int_0^1 n\, dy \exp\left\{n\left[\ln(a+1) - \frac{(a+1)^2}{2a}(y-y_{\max})^2 + \cdots\right]\right\} \tag{3.33}$$

Because the factor of n in the exponential is so large, the above quadratic approximation gives an accurate expression for the integral, leading to

$$C_{p;n} = a^n[F(n) + (-1)^n G(n)] = \frac{1}{3^n}(1+a)^n \times \left[pF\left(\frac{an}{1+a}\right) \pm (1-p)\, G\left(\frac{an}{1+a}\right)\right] \tag{3.34}$$

which implies that

$$a = 1/2 \tag{3.35}$$

$$F(n) = pF(n/3) \tag{3.36}$$

$$G(n) = (1-p)\, G(n/3) \tag{3.37}$$

The value of a comes from the fact that the distribution ends at $x = 1/2$. The general solution for the equation for $F(n)$ is

$$F(n) = \sum_{m=-\infty}^{\infty} f_m n^{\phi_m} \tag{3.38}$$

where

$$\phi_m = \frac{\ln p}{\ln 3} + \frac{2\pi i m}{\ln 3} \tag{3.39}$$

and the f_m are coefficients which are yet to be determined. This expression may also be written as $n^{\ln p/\ln 3}$ multiplied by a Fourier series in $\ln n$. The expression for $G(n)$ follows similarly:

$$G(n) = \sum_{m=-\infty}^{\infty} g_m n^{\gamma_m} \tag{3.40}$$

where

$$\gamma_m = \frac{\ln(1-p)}{\ln 3} + \frac{2\pi i m}{\ln 3} \tag{3.41}$$

Figures 3 and 4 show numerical plots of the Fourier series for F and G, that is, these functions with the power law dependence removed. The oscillatory behavior is quite clear, as are the $1/n$ corrections for small n, which are negligible in the large-n limit of the above calculation.

Now we use an expression for the potential found in the previous subsection and the fact that the potential near the end of the fractal, where the series (3.20) is barely convergent, is closely related to the $n \to \infty$ limit of the $C_{p;n}$, to find the f_m and g_m coefficient, is closely related to the $n \to \infty$ limit of the $C_{p;n}$, to find the f_m and g_m coefficients. We begin with Eq. (3.20), set $y = 0$, and perform the multiple derivative, to obtain

$$V_p\left(x + \frac{1}{2}, 0\right) = \sum_{n=0}^{\infty} \frac{C_{p;n}}{(x+1/2)^{n+1}} \tag{3.42}$$

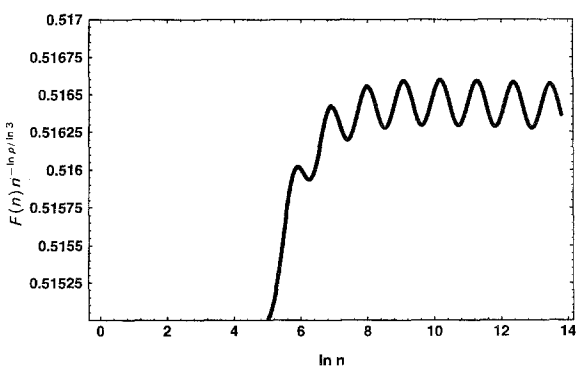

Fig. 3. A plot of $F(n)\,n^{-\ln p/\ln 3}$, where $F(n)$ is defined in Eq. (3.26).

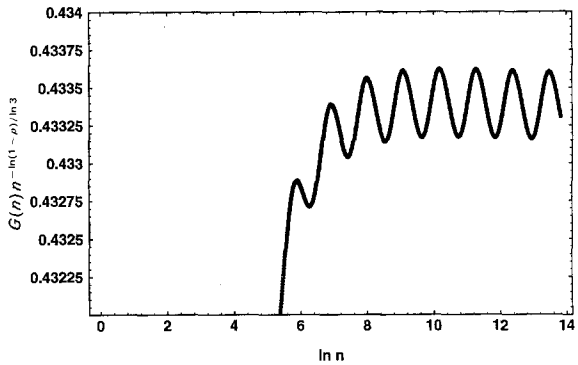

Fig. 4. A plot of $G(n)\, n^{-\ln(1-p)/\ln 3}$, where $G(n)$ is defined in Eq. (3.26).

This expression is then Mellin transformed with respect to x, and the $C_{p;n}$ expanded as in Eq. (3.26) to give

$$V_p\left(x+\frac{1}{2}, 0\right) = \frac{1}{2\pi i}\int_{c-i\infty}^{c+i\infty} ds\, x^{-s} \sum_{n=0}^{\infty} \sum_{m=-\infty}^{\infty} f_m n^{\phi_m} \left(\frac{1}{2}\right)^{s-n-1} \times \frac{\Gamma(s)\,\Gamma(n+1-s)}{\Gamma(n+1)} \tag{3.43}$$

where the signs due to odd and even n have been averaged over. Here, we are only considering the terms which are divergent in the $x \to 0$ limit, thus the terms for small n, and the part of $C_{p;n}$ neglected in the previous calculation do not contribute. Stirling's formula (3.28) leads to

$$\Gamma(n+1-s)/\Gamma(n+1) = n^{-s}(1+O(1/n)) \tag{3.44}$$

Dropping the $n=0$ term, which was just a constant in the original sum, the sum over n is now simply

$$\sum_{n=1}^{\infty} n^{\phi_m - s} = \zeta(s-\phi_m) \tag{3.45}$$

where $\zeta(z)$ is the Reimann zeta function, which has a pole of residue 1 at $z=1$. Thus, closing the contour to the left, we obtain

$$V_p(x+1/2, 0) = \text{const} + \sum_{m=\infty}^{\infty} \Gamma(s_m)\, f_m (1/2)^{s_m - 1}\, x^{-s_m} \tag{3.46}$$

where

$$s_m = 1 + \frac{\ln p}{\ln 3} + \frac{2\pi i m}{\ln 3} \tag{3.47}$$

This may be compared with Eq. (3.21) to give

$$f_m = \frac{1}{\ln 3} \frac{1-p}{p} 2^{s_m - 1} \sum_{n=0}^{\infty} \frac{C_{p;n}}{n!} \Gamma(n+1-s_m) \left(\frac{2}{5}\right)^{n+1-s_m} \tag{3.48}$$

The corresponding expression for g_m is found by replacing p by $1-p$ in the above derivation; the $C_{1-p,n}$ give the alternating minus signs [see Eq. (3.25)] which single out the g_m from the original sum. The result is exactly the same expression, but with p replaced by $1-p$. This symmetry ensures that in the case $p = 1/2$ all the odd moments are zero.

3.4. Fourier Transform

Now we turn to the Fourier transform of the distribution. This is given as [Eq. (2.15)]

$$\begin{aligned} \tilde{C}_p(k) &= \prod_{j=1}^{\infty} [(1-p)\, e^{-i3^{-j}k} + p e^{i3^{-j}k}] \\ &= \prod_{j=1}^{\infty} [\cos 3^{-j}k + i(2p-1) \sin 3^{-j}k] \end{aligned} \tag{3.49}$$

The product converges for all complex values of k, and is thus a perfectly well-behaved analytic function. It gives us a representation for the original distribution

$$C_p(x) = \int_{-\infty}^{\infty} \frac{dk}{2\pi} e^{-ikx} \prod_{j=1}^{\infty} [\cos 3^{-j}k + i(2p-1) \sin 3^{-j}k] \tag{3.50}$$

as well as the moments [Eq. (2.17)]

$$C_{p;n} = (-i)^n \frac{\partial^n}{\partial k^n} \prod_{j=1}^{\infty} [\cos 3^{-j}k + i(2p-1) \sin 3^{-j}k] \Big|_{k=0} \tag{3.51}$$

Generally, random fractals are characterized by a noninteger power law decline of the power spectrum as $k \to \infty$, and this property has been used to define the concept of Fourier dimension.[16] However, for exactly self-similar distributions, this limit does not exist, due to the presence of long-range correlations. In the above case, a value of k equal to $3^q \pi$ for an

arbitrarily large integer q results in the first q terms in the product being equal to 1, so that

$$\tilde{C}_p(3^q\pi) = \tilde{C}_p(\pi) \tag{3.52}$$

Thus the above expression does not strictly tend to zero for large k. We can, however find its "average" behavior by cutting off the product when the argument of the trigonometric functions is of order 1, and for the remaining terms using the geometric mean of the absolute value of $\cos x + i(2p-1)\sin x$,

$$\exp\left\{\frac{1}{2\pi}\int_0^{2\pi} \ln[\cos^2 x + (2p-1)^2 \sin^2 x]^{1/2}\, dx\right\} = \max(p, 1-p) \tag{3.53}$$

so that the power spectrum has the "averaged" law

$$|\tilde{C}_p(k)|^2 \sim k^{2 \ln \max(p,\, 1-p)/\ln 3} \tag{3.54}$$

For the purposes of the Fourier transform, the effective dimension is thus also the smallest dimension $(-\ln p/\ln 3)$ applicable to this distribution. In other words, the power spectrum decreases at the slowest rate available to it.

3.5. SUMMARY

The binomial distribution on the Cantor set may be treated in an analogous fashion to the uniform case,[13] but shows much additional structure. The dimension of the support of the distribution, ln 2/ln 3, plays no discernible role in the structure of the potential, the moments, or the Fourier transform. Rather, the structure of the potential is governed by an effective dimension which depends on the point near which the potential is measured. This effective dimension varies between $-\ln p/\ln 3$ and $-\ln(1-p)/\ln 3$. The asymptotic form of the moments has terms corresponding to each of these endpoints, but no intermediate effective dimension. The behavior of the Fourier transform is apparently dominated by only the minimum of these two values, although the other value is undoubtably hidden in its deeper structure.

4. THE MENGER SPONGE

4.1. Definition

The purpose of this section is to investigate the effects of increasing the dimension of the space in which the fractal is embedded, while having as

little other complication as possible. Thus the distributions considered here will be uniform in the sense defined in Section 2 and the transformations do not contain any rotations. Probably the simplest three-dimensional fractal is the outer product of three Cantor sets. The uniform distribution on this set is simply given by

$$C_{1/2}(x)\, C_{1/2}(y)\, C_{1/2}(z) \tag{4.1}$$

The presence of complicated square roots makes the potential difficult to calculate in three dimensions; see, for example, the treatment of the von Koch snowflake given in the next section. The moments and Fourier transform of this distribution, however, are readily obtainable from those of the uniform Cantor distribution, and thus do not shed much light on the properties of more general fractals, which do not separate in this way. It is clear that a slightly more complicated example is needed.

Probably the best-known fractal in three dimensions is the Menger sponge. This is closely related to the Cantor set, but not simply the outer product of three Cantor sets. It is defined by taking a cube of length 1, and centered on the origin, dividing it into 27 smaller cubes, and accepting only the 20 of those which contain the edges of the original cube—see Fig. 5.

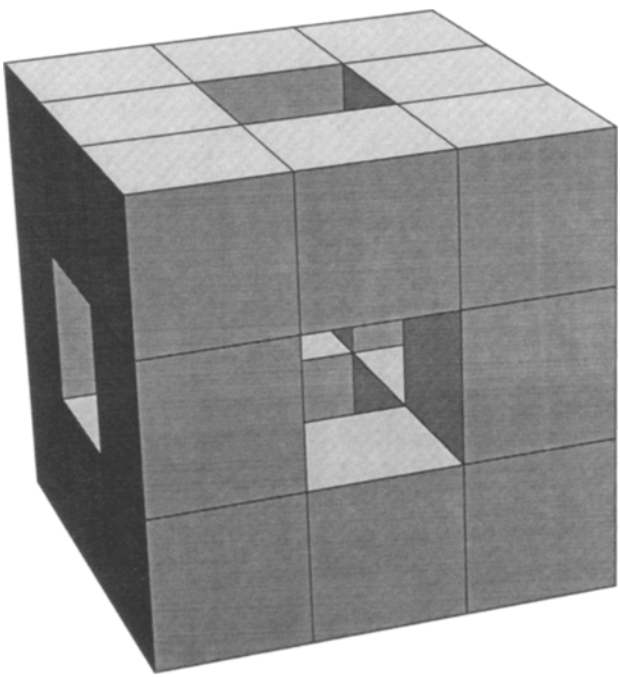

Fig. 5. The first step in the construction of the Menger sponge. The large cube has vertices at $\pm 1/2$.

This process is continued for each of the smaller cubes, and so on. The result is rather difficult to draw on a computer, and we refer the reader to p. 145 of Mandelbrot,[16] which was in turn copied from an earlier book! Mathematically, however, the Menger sponge is quite easy to define. Using the results in Section 2, we obtain the dimension of the set (ln 20/ln 3) and also a recursion relation for the uniform distribution on the Menger sponge, $M(x, y, z)$:

$$\begin{aligned} M(x, y, z) = \frac{27}{20} [&M(X_+, Y_+, Z_+) + M(X_+, Y_+, Z) + M(X_+, Y_+, Z_-) \\ &+ M(X_+, Y, Z_+) + M(X_+, Y, Z_-) + M(X_+, Y_-, Z_+) \\ &+ M(X_+, Y_-, Z) + M(X_+, Y_-, Z_-) + M(X, Y_+, Z_+) \\ &+ M(X, Y_+, Z_-) + M(X, Y_-, Z_+) + M(X, Y_-, Z_-) \\ &+ M(X_-, Y_+, Z_+) + M(X_-, Y_+, Z) + M(X_-, Y_+, Z_-) \\ &+ M(X_-, Y, Z_+) + M(X_-, Y, Z_-) + M(X_-, Y_-, Z_+) \\ &+ M(X_-, Y_-, Z) + M(X_-, Y_-, Z_-)] \end{aligned} \tag{4.2}$$

where

$$\begin{aligned} X_+ &= 3x + 1, & X &= 3x, & X_- &= 3x - 1 \\ Y_+ &= 3y + 1 & Y &= 3y & Y_- &= 3y - 1 \\ Z_+ &= 3z + 1 & Z &= 3z & Z_- &= 3z - 1 \end{aligned} \tag{4.3}$$

4.2. Moments

The moments M_{ijk} follow the symmetries of the distribution, that is, they are totally symmetric in i, j, and k, and are zero if one or more of the indices is odd. The above recursion relation for the distribution leads to the following expression for the even moments:

$$M_{ijk} = \frac{1}{5} \frac{1}{3^{i+j+k} - 1} \sum_{a,b,c} M_{abc} \binom{i}{a} \binom{j}{b} \binom{k}{c} (2 + \delta_{ia} + \delta_{jb} + \delta_{kc}) \tag{4.4}$$

where the sum is over all even values of a, b, and c permitted by the binomial coefficients except for the term in which $a = i$, $b = j$, and $c = k$, and δ_{mn} refers to the Kronecker delta, equal to 1 if $m = n$ and zero otherwise. Some values of the coefficients are given in Table II.

The asymptotic properties of the moments for large i, j, and k are obtained using a similar procedure to that of the previous section. The δ_{mn}

Table II. Moments of the Menger Sponge

M_{000}	1
M_{002}	1/10
M_{004}	2/125
M_{022}	19/2000
M_{006}	137/45500
M_{024}	1373/910000
M_{222}	1507/1820000

only contribute at the endpoints of the sum, and thus are negligible in this limit. If the ansatz

$$M_{ijk} = a^{i+j+k} f(i) f(j) f(k) \tag{4.5}$$

is substituted into the above expression, the triple sum separates. Following the same procedure as in the previous section, the binomial coefficients are simplified using Stirling's formula, the sum is written as an integral, and the integral is performed using the method of steepest descents. The result is

$$a = 1/2 \tag{4.6}$$

$$f(n) = 20^{-1/3} f(n/3) \tag{4.7}$$

which leads to an expression of the form

$$f(n) = \sum_{m=-\infty}^{\infty} f_m n^{\phi_m} \tag{4.8}$$

where

$$\phi_m = -\frac{\ln 20}{3 \ln 3} + \frac{2\pi i m}{\ln 3} \tag{4.9}$$

Again the 1/2 is due to the size of the fractal, but now there is an extra factor of 3 in the ϕ_m. It appears likely that this factor is the embedding dimension E; however, as the section on the moments of the von Koch snowflake shows, the situation is not this simple. The coefficients f_m cannot be determined at this point by a similar means to those of the binomial Cantor distribution, since the potential has not been evaluated.

4.3. Fourier Transform

The Fourier transform of the Menger sponge is given by [Eq. (2.15)]

$$\tilde{M}(k_x, k_y, k_z) = \prod_{j=1}^{\infty} \tfrac{1}{5}(2\xi\eta\zeta + \xi\eta + \eta\zeta + \zeta\xi) \tag{4.10}$$

where

$$\xi = \cos(3^{-j}k_x)$$

$$\eta = \cos(3^{-j}k_y)$$

$$\zeta = \cos(3^{-j}k_z)$$

This is quite similar to the Fourier transform of the outer product of three Cantor sets,

$$\tilde{C}_{1/2}(k_x)\,\tilde{C}_{1/2}(k_y)\,\tilde{C}_{1/2}(k_z) = \prod_{j=1}^{\infty} \xi\eta\zeta \tag{4.11}$$

but has the factor of 5 characteristic of the Menger sponge, while still keeping the symmetry between x, y, and z. Like the binomial Cantor distribution, it does not tend to zero for large k_x, k_y, and/or k_z. All but a small number of terms in the product are close to 1 if k_x, k_y, and k_z are all of the form $3^q\pi$ or zero, where q is a positive integer.

As in the previous section, the approximate form of $\tilde{M}^2$ for large arguments may be found by replacing terms in the product by their geometric mean; in this case, however, the integrals must be performed numerically. Without loss of generality we assume that $k_x \geqslant k_y \geqslant k_z$. The product then breaks up into several groups of terms, defined as follows:

1. $3^{-j}k_z \geqslant 1$. The geometric mean of the square of the terms in Eq. (4.10),

$$\begin{aligned}\exp(I_3) &= \exp\left(\frac{1}{(2\pi)^3}\int_0^{2\pi}\int_0^{2\pi}\int_0^{2\pi} \ln\left\{\left[\frac{1}{5}(2\cos x\cos y\cos z\right.\right.\right.\\ &\qquad \left.\left.\left. + \cos x\cos y + \cos y\cos z + \cos z\cos x)\right]^2\right\} dx\,dy\,dz\right)\\ &= 0.00917 \pm 4\times 10^{-5}\end{aligned} \tag{4.12}$$

2. $3^{-j}k_z \leqslant 1$ and $3^{-j}k_y \geqslant 1$. Now, one of the cosines is approximately one, so that the appropriate expression is

$$\begin{aligned}\exp(I_2) &= \exp\left(\frac{1}{(2\pi)^2}\int_0^{2\pi}\int_0^{2\pi} \ln\left\{\left[\frac{1}{5}(3\cos x\cos \mathrm{y} + \cos x + \cos y)\right]^2\right\} dx\,dy\right)\\ &= 0.0290 \pm 1\times 10^{-4}\end{aligned} \tag{4.13}$$

3. $3^{-j}k_y \leqslant 1$ and $3^{-j}k_x \geqslant 1$. With only one of the cosines varying, the integral can be obtained analytically as

$$\exp(I_1) = \exp\left(\frac{1}{2\pi}\int_0^{2\pi} \ln\left\{\left[\frac{1}{5}(4\cos x + 1)\right]^2\right\} dx\right) = \frac{4}{25} \tag{4.14}$$

4. $3^{-j}k_x \leqslant 1$. These terms are approximately equal to 1.

Substituting these expressions into the product, evaluating the number of terms corresponding to each case gives

$$\tilde{M}(k_x, k_y, k_z)^2 = Z^{I_3/\ln 3} Y^{I_2/\ln 3} X^{I_1/\ln 3} \tag{4.15}$$

where

$$\begin{aligned} Z &= \max(k_z, 1) \\ Y &= \max(k_y/Z, 1) \\ X &= \max(k_x/Y, 1) \end{aligned} \tag{4.16}$$

Unlike the one-dimensional case, this expression does not contain the dimension of the fractal distribution explicitly. Even the part involving I_1 is modified

$$\frac{I_1}{\ln 3} = -\frac{2\ln(20/8)}{\ln 3} \tag{4.17}$$

with the presence of the 8 somewhat mysterious.

5. THE VON KOCH SNOWFLAKE

5.1. Definition

Finally we consider the von Koch snowflake, which, in addition to being in two dimensions, has transformations which contain rotations. The snowflake is constructed by the following iterative procedure: Take an equilateral triangle, which we will take to have side length 1, centered on the origin, and with its apex on the y axis; replace each side by the construction shown in Fig. 6, in which each of the new sides has a length 1/3 of the original; repeat this for each of the 12 sides of the new figure, and so on. The result is shown in Fig. 7. Since each part of the fractal consists of four copies of itself reduced by a factor 3, the dimension of the fractal is ln 4/ln 3.

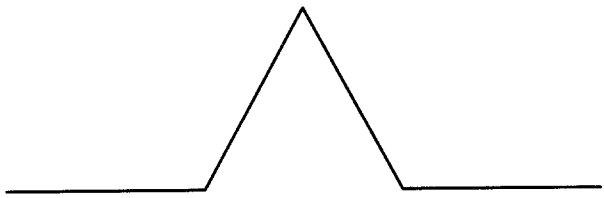

Fig. 6. In the construction of the von Koch snowflake, each edge of an equilateral triangle is replaced by this figure. Each of the resulting 12 edges is replaced by this figure, ad infinitum.

There are a number of possible choices for the defining transformations for the von Koch snowflake. The most obvious is to split it into three sections, each of which is given by four copies of itself. If the snowflake must be treated as a whole, it is possible to write the recursion relation for the uniform distribution $K(x, y)$ in terms of six copies of itself reduced by $1/3$ minus a single copy rotated by $\pi/6$ and reduced by $1/\sqrt{3}$. The most economical in terms of the number of transformations, however, is to split the snowflake into three sections, as above, but use only two transformations, noting that the outside of the snowflake is similar to the inside.

Let the uniform distribution on the upper third of the fractal with normalization $1/3$ be denoted by $k(x, y)$. The treatment in Section 2 gives the relation

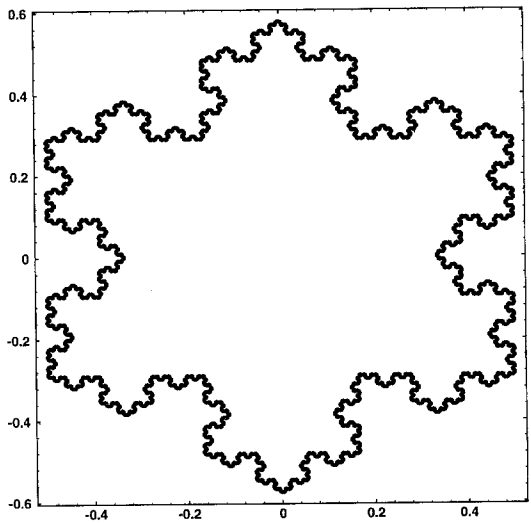

Fig. 7. The von Koch snowflake. The side length of one of the large triangles is 1. Note that the inside of the snowflake is similar to the outside.

$$k(x, y) = \frac{3}{2}\left[k\left(-\frac{3x}{2}+\frac{\sqrt{3}\,y}{2}, -\frac{\sqrt{3}\,x}{2}-\frac{3y}{2}+\frac{2\sqrt{3}}{3}\right)\right.$$
$$\left.+k\left(\frac{3x}{2}+\frac{\sqrt{3}\,y}{2}, \frac{\sqrt{3}\,x}{2}-\frac{3y}{2}+\frac{2\sqrt{3}}{3}\right)\right] \tag{5.1}$$

The distribution for the entire snowflake is then given by

$$K(x, y) = k(x, y) + k\left(-\frac{x}{2}+\frac{\sqrt{3}\,y}{2}, -\frac{\sqrt{3}\,x}{2}-\frac{y}{2}\right)$$
$$+k\left(-\frac{x}{2}-\frac{\sqrt{3}\,y}{2}, \frac{\sqrt{3}\,x}{2}-\frac{y}{2}\right) \tag{5.2}$$

so that

$$\int_{-\infty}^{\infty}\int_{-\infty}^{\infty} K(x, y)\,dx\,dy = 1 \tag{5.3}$$

5.2. Potential

The recursion relation for the potential of the upper third of the distribution in three dimensions ($\beta = 1$) is given by [Eq. (2.10)]

$$v(x, y, z) = \frac{\sqrt{3}}{2}\left[v\left(-\frac{3x}{2}+\frac{\sqrt{3}\,y}{2}, -\frac{\sqrt{3}\,x}{2}-\frac{3y}{2}+\frac{2\sqrt{3}}{3}, \sqrt{3}\,z\right)\right.$$
$$\left.+v\left(\frac{3x}{2}+\frac{\sqrt{3}\,y}{2}, \frac{\sqrt{3}\,x}{2}-\frac{3y}{2}+\frac{2\sqrt{3}}{3}, \sqrt{3}\,z\right)\right] \tag{5.4}$$

This expression is used to evaluate the potential near the fractal in terms of its values at a greater distance from the origin. At large distances from the fractal the series obtained by expanding Eq. (2.9) in a Taylor series,

$$v(x, y, z) = \sum_{m=0}^{\infty}\sum_{n=0}^{\infty} \frac{k_{m,n}}{m!\,n!}\frac{\partial^m}{\partial x'^m}\frac{\partial^n}{\partial y'^n}$$
$$\times \frac{1}{[(x-x')^2+(y-y')^2+z^2]^{1/2}}\bigg|_{x'=y'=0} \tag{5.5}$$

where $k_{m,n}$ are the moments of the $k(x, y)$ distribution, defined in the usual way by

$$k_{m,n} = \int_{-\infty}^{\infty}\int_{-\infty}^{\infty} k(x, y)\,x^m y^n\,dx\,dy \tag{5.6}$$

The moments are studied more fully in the next subsection.

The potential of the full snowflake $V(x, y, z)$ is given in terms of v as

$$V(x, y, z) = v(x, y, z) + v\left(-\frac{x}{2} + \frac{\sqrt{3}\,y}{2}, -\frac{\sqrt{3}\,x}{2} - \frac{y}{2}, z\right) + v\left(-\frac{x}{2} - \frac{\sqrt{3}\,y}{2}, \frac{\sqrt{3}\,x}{2} - \frac{y}{2}, z\right) \tag{5.7}$$

This potential is plotted in Fig. 8.

Now we use the Mellin transform technique of Section 3 to investigate $V(x, y, z)$ along the y axis above the uppermost point of the fractal at $(0, \sqrt{3}/3, 0)$. A direct application of the relation (5.4) gives

$$\begin{aligned} v\left(0, \frac{\sqrt{3}}{3} + y, 0\right) &= \sqrt{3}\, v\left(\frac{1+\sqrt{3}\,y}{2}, \frac{\sqrt{3}-9y}{6}\right) \\ &= \frac{3\sqrt{3}}{4}\left[v\left(\frac{1+3\sqrt{3}\,y}{2}, \frac{\sqrt{3}-27y}{6}\right)\right. \\ &\quad \left. + v\left(1+3\sqrt{3}\,y, \frac{2}{\sqrt{3}}\right) + \frac{2}{\sqrt{3}}\, v\left(1, \frac{2}{\sqrt{3}} + 3y\right)\right] \\ &= \sqrt{3} \sum_{j=1}^{\infty} \left(\frac{3}{4}\right)^j \left[v\left(1+3^{j+1/2}y, \frac{2}{\sqrt{3}}\right)\right. \\ &\quad \left. + \frac{2}{\sqrt{3}}\, v\left(1, \frac{2}{\sqrt{3}} + 3^j y\right)\right] \end{aligned} \tag{5.8}$$

From this point the analysis is similar to that of Section 3; Eq. (5.5) is substituted for v and the expression involving y is written as the inverse Mellin transform of its Mellin transform, specifically,

$$\begin{aligned} v\left(0, \frac{\sqrt{3}}{3} + y, 0\right) &= \sqrt{3} \sum_{j=1}^{\infty} \left(\frac{3}{4}\right)^j \sum_{m=0}^{\infty} \sum_{n=0}^{\infty} \frac{k_{m,n}}{m!\,n!} \frac{\partial^m}{\partial x'^m} \frac{\partial^n}{\partial y'^n} \frac{1}{2\pi i} \\ &\quad \times \int_{c-i\infty}^{c+i\infty} ds\, y^{-s} \frac{\pi}{\sin \pi s} \left[3^{-j-1/2}(3^{-j-1/2}C)^{s-1} P_{s-1}\left(\frac{A}{C}\right)\right. \\ &\quad \left. + \frac{2}{\sqrt{3}} 3^{-j}(3^{-j}C)^{s-1} P_{s-1}\left(\frac{B}{C}\right)\right]\Bigg|_{x'=y'=0} \end{aligned} \tag{5.9}$$

where

$$\begin{aligned} &0 < c < 1 \\ &A = 1 - x' \\ &B = 2/\sqrt{3} - y' \\ &C = (A^2 + B^2)^{1/2} \end{aligned} \tag{5.10}$$

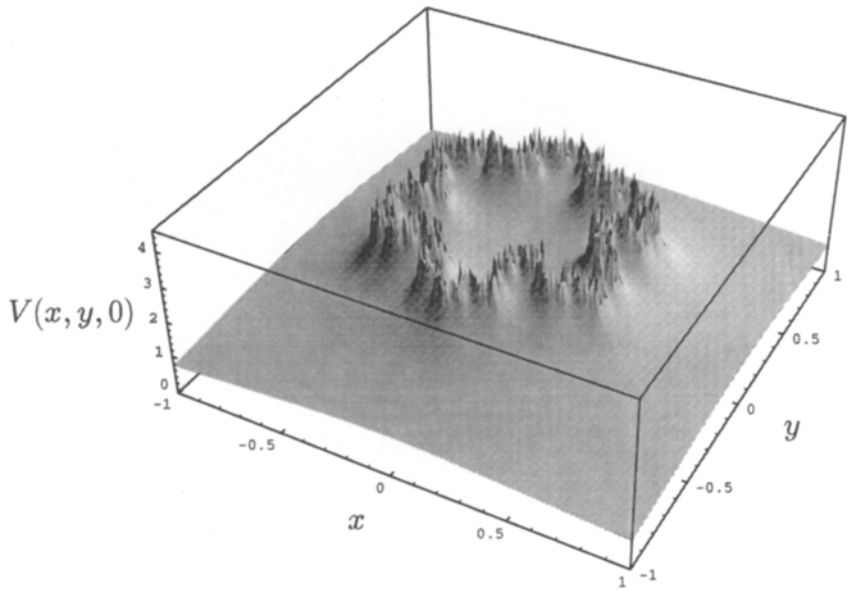

Fig. 8. The potential of the von Koch snowflake, defined using Eq. (2.9) with $\beta = 1$.

and the $P_{s-1}(z)$ are Legendre functions of the first kind, reducing to Legendre polynomials for the case s an integer, but not for the case of interest at $s = s_k$ (see below). As for the binomial Cantor distribution, the sum over j is a geometric series, leading to poles at

$$s_k = 1 - \frac{\ln 4}{\ln 3} + \frac{2\pi i k}{\ln 3} \tag{5.11}$$

for all integers k. The $\sin \pi s$ in the denominator generates poles for all integers s. Closing the contour to the left thus gives an expression including a series of terms of the form $y^{\ln 4/\ln 3 - 1}$ multiplied by oscillatory terms, plus a power series in y beginning with a constant. It thus has the same form as the potential from the Cantor set, although the coefficients are more difficult to calculate. The full potential V also contains contributions from the other two-thirds of the snowflake. The contributions due to each third are equal, and given by [see Eqs. (5.5), (5.7)]

$$\begin{aligned} &v\left(\frac{1}{2} + \frac{\sqrt{3}y}{2}, -\frac{\sqrt{3}}{6} - \frac{y}{2}, 0\right) \\ &\quad = \sum_{m=0}^{\infty} \sum_{n=0}^{\infty} \frac{k_{m,n}}{m!\, n!} \frac{\partial^m}{\partial x'^m} \frac{\partial^n}{\partial y'^n} \\ &\qquad \times \frac{1}{[(1/2 + \sqrt{3}y/2 - x')^2 + (-\sqrt{3}/6 - y/2 - y')^2]^{1/2}} \Bigg|_{x' = y' = 0} \end{aligned} \tag{5.12}$$

which is then Mellin transformed in the same way as the previous expression. The final result for the potential near the uppermost point of the snowflake is

$$
\begin{aligned}
V\left(0, \frac{\sqrt{3}}{3}+y, 0\right) &= v\left(0, \frac{\sqrt{3}}{3}+y, 0\right) + 2v\left(\frac{1}{2}+\frac{\sqrt{3}y}{2}, -\frac{\sqrt{3}}{6}-\frac{y}{2}, 0\right) \\
&= \frac{\sqrt{3}\,\pi}{\ln 3} \sum_{k=-\infty}^{\infty} \frac{y^{-s_k}}{\sin \pi s_k} \sum_{m=0}^{\infty} \sum_{n=0}^{\infty} \frac{k_{m,n}}{m!\,n!} \frac{\partial^m}{\partial x'^m} \frac{\partial^n}{\partial y'^n} \\
&\quad \times \left\{ C^{s_k-1} \left[3^{-s_k/2} P_{s_k-1}\left(\frac{A}{C}\right) + \frac{2}{\sqrt{3}} P_{s_k-1}\left(\frac{B}{C}\right) \right] \right\} \Bigg|_{x'=y'=0} \\
&\quad + \sqrt{3} \sum_{q=0}^{\infty} \frac{(-1)^q y^q}{3^{-q-1}4-1} \sum_{n=0}^{\infty} \frac{k_{m,n}}{m!n!} \frac{\partial^m}{\partial x'^m} \frac{\partial^n}{\partial y'^n} \\
&\quad \times \left\{ C^{-q-1} \left[3^{q/2} P_q\left(\frac{A}{C}\right) + \frac{2}{\sqrt{3}} P_q\left(\frac{B}{C}\right) \right] \right\} \Bigg|_{x'=y'=0} \\
&\quad + 2 \sum_{q=0}^{\infty} (-1)^q y^q \sum_{n=0}^{\infty} \frac{k_{m,n}}{m!n!} \frac{\partial^m}{\partial x'^m} \frac{\partial^n}{\partial y'^n} \\
&\quad \times \left\{ E^{-q-1} P_q\left(\frac{D}{E}\right) \right\} \Bigg|_{x'=y'=0}
\end{aligned}
\tag{5.13}
$$

where A, B, C, and s_k are defined as previously, and

$$
\begin{aligned}
D &= \frac{\sqrt{3}}{3} - \frac{\sqrt{3}\,x'}{2} + \frac{y'}{2} \\
E &= \left[\left(\frac{1}{2} - x'\right)^2 + \left(\frac{\sqrt{3}}{6} + y'\right)^2 \right]^{1/2}
\end{aligned}
\tag{5.14}
$$

and the relation

$$
P_{-q-1}(z) = P_q(z) \tag{5.15}
$$

has been used. The first few terms in the above expression for the coefficients of powers of y were evaluated numerically. With the exception of the coefficient of $y^{\ln 4/\ln 3 - 1}$, which converged rapidly to 3.7481, all of the series converged quite slowly. As in the case of the binomial Cantor distribution, however, the coefficient of $y^{\ln 4/\ln 3 - 1 - 2\pi i/\ln 3}$ is of order 10^{-6}, showing that the oscillations in $\ln y$ are again small in this case.

Closing the contour to the right in Eq. (5.9) gives the large-y expansion. The Legendre polynomials are finite, cutting off the sum over m and

n. Thus the coefficients of powers of $1/y$ are known combinations of rational numbers and $\sqrt{3}$,

$$V\left(0, \frac{\sqrt{3}}{3}+y, 0\right)=\sum_{q=1}^{\infty} y^{-q}(-1)^{q+1} \sum_{m=0}^{\infty} \sum_{n=0}^{\infty} \frac{k_{m,n}}{m!\,n!} \frac{\partial^m}{\partial x'^m} \frac{\partial^n}{\partial y'^n}$$
$$\times\left\{\frac{\sqrt{3}\,C^{q-1}}{3^{q-1}4-1}\left[3^{-q/2}P_{q-1}\left(\frac{A}{C}\right)+\frac{2}{\sqrt{3}}P_{q-1}\left(\frac{B}{C}\right)\right]\right.$$
$$\left.+2E^{q-1}P_{q-1}\left(\frac{D}{E}\right)\right\}\Bigg|_{x'=y'=0}$$
$$=\frac{1}{y}-\frac{1}{\sqrt{3}\,y^2}+\frac{7}{18y^3}-\frac{1}{2\sqrt{3}\,y^4}+\frac{463}{2016y^5}-\cdots \tag{5.16}$$

5.3. Moments

The moments of the upper third of the snowflake $k_{m,n}$ and of the entire snowflake $K_{m,n}$ are defined in the usual way,

$$k_{m,n}=\int_{-\infty}^{\infty}\int_{-\infty}^{\infty} k(x, y)\, x^m y^n\, dx\, dy \tag{5.17}$$

$$K_{m,n}=\int_{-\infty}^{\infty}\int_{-\infty}^{\infty} K(x, y)\, x^m y^n\, dx\, dy \tag{5.18}$$

The $k_{m,n}$ obey a recursion relation obtained by substituting Eq. (5.1) into Eq. (5.17),

$$k_{m,n}=\sum_{m_1=0}^{m}\sum_{m_2=0}^{m-m_1}\sum_{n_1=0}^{n}\sum_{n_2=0}^{n-n_1}\frac{m!}{m_1!\,m_2!(m-m_1-m_2)!}$$
$$\times\frac{n!}{n_1!\,n_2!(n-n_1-n_2)!}(-1)^{m_1+m_2+n_2}\left(\frac{1}{2}\right)^{m_1+m_2+n_1+n_2}$$
$$\times\left(\frac{1}{\sqrt{3}}\right)^{2m-2m_1-m_2+n-n_2} k_{m_1+n_1, m_2+n_2} \tag{5.19}$$

This is a set of linear equations involving all of the $k_{m,n}$ up to a particular value of $m+n$. The "mixing" of the recursion formulas in this way is due to the rotations in the original transformation. It requires a much larger amount of calculation to evaluate these moments than for the case without rotations, and it is also much more difficult to determine analytically the

asymptotic behavior as m, $n \to \infty$. The moments for the whole snowflake are obtained by substituting Eq. (5.2) into Eq. (5.18),

$$K_{m,n} = k_{m,n} + \sum_{m'=0}^{m} \sum_{n'=0}^{n} [(-1)^{m+n-n'} + (-1)^{n+m'}] \times \left(\frac{1}{2}\right)^{m+n} (\sqrt{3})^{m-m'+n'} k_{m'+n',m+n-m'-n'} \tag{5.20}$$

The first few $k_{m,n}$ and $K_{m,n}$ are tabulated in Table III. Note that the symmetries of the distributions impose certain conditions on the moments. Both $k(x, y)$ and $K(x, y)$ have the y axis as a line of symmetry, so all of the moments with m odd are equal to zero. Similarly the $K_{m,n}$ with n odd are also equal to zero. The full von Koch distribution is invariant under $\pi/3$ rotations. A little algebra shows that this implies $K_{0,2} = K_{2,0}$ and $K_{4,0} = K_{0,4} = 3K_{2,2}$. The pattern does not continue: $K_{0,6} \neq K_{6,0}$.

Although the authors cannot see a method of determining the asymptotic form of either the $k_{m,n}$ or the $K_{m,n}$, it is possible to make hypotheses based on the results of the previous sections and test them numerically. Our computer resources permit us to go only as far as $m + n = 100$. We restrict ourselves here to the case $m = 0$ or $n = 0$. The dominant factor in $K_{m,0}$ is of the form a^m, where a is the greatest extent of the distribution in the x direction, that is, 1/2. Based on the results from the

Table III. Moments of the von Koch Snowflake

m, n	$k_{m,n}$	$K_{m,n}$
0, 0	1/3	1
0, 1	$2\sqrt{3}/27$	0
0, 2	7/135	1/9
2, 0	1/45	1/9
0, 3	$4\sqrt{3}/315$	0
2, 1	$4\sqrt{3}/315$	0
0, 4	35737/3662820	5/252
2, 2	59/23940	5/756
4, 0	1201/406980	5/252
0, 5	$2855\sqrt{3}/1098846$	0
2, 3	$2687\sqrt{3}/5494230$	0
4, 1	$989\sqrt{3}/1831410$	0
0, 6	19838747/9253504260	13669/3174444
2, 4	24886319/83281538340	2141/3174444
4, 2	8304973/27760512780	149/151164
6, 0	167641/342722380	1409/352716

Menger sponge, we would expect a factor of the form $m^{-\ln 4/2 \ln 3}$, where the $\ln 4/\ln 3$ is the dimension of the fractal, and the 2 is the embedding dimension E. Thus a function

$$K_1(m) = K_{m,0} 2^m m^{\ln 2/\ln 3} \tag{5.21}$$

is plotted against m. The graph is quite flat, converging to approximately 0.857, as shown in Fig. 9, indicating that this form is approximately correct. Similarly, in the y direction, we might expect a similar form, with a equal to $1/\sqrt{3}$. This is not the case, and it appears that the correct quantity to be plotted is in fact

$$K_2(n) = K_{0,n} 3^{n/2} n^{\ln 4/\ln 3} \tag{5.22}$$

which also gives a flat graph, converging to approximately 1.382, as shown in Fig. 9. The factor of 2 difference between these two cases is simply a numerical observation; it is hoped that further investigation into the structure of these moments will shed more light on this interesting factor.

5.4. Fourier Transform

The presence of rotations makes it difficult to write an explicit expression such as Eq. (2.15) for the Fourier transform of the k distribution, $\tilde{k}(\mathbf{k})$; however, there are a few results which can be deduced directly from the recursion relation, Eq. (2.14),

$$\begin{aligned}\tilde{k}(k_x, k_y) = \frac{1}{2}\Bigg[& e^{i(k_x/3 + k_y/\sqrt{3})}\tilde{k}\left(-\frac{k_x}{2} + \frac{k_y}{2\sqrt{3}}, -\frac{k_x}{2\sqrt{3}} - \frac{k_y}{2}\right) \\ & + e^{i(-k_x/3 + k_y/\sqrt{3})}\tilde{k}\left(\frac{k_x}{2} + \frac{k_y}{2\sqrt{3}}, \frac{k_x}{2\sqrt{3}} - \frac{k_y}{2}\right)\Bigg]\end{aligned} \tag{5.23}$$

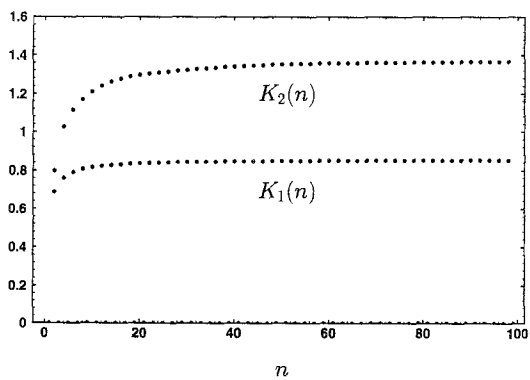

Fig. 9. The asymptotic behavior of the moments of the von Koch distribution. See Eqs. (5.21), (5.22).

A power series expansion for $\tilde{k}$ around $\mathbf{k}=0$ may be obtained by expanding the exponential in Eq. (2.13) in its power series to obtain

$$\tilde{k}(k_x, k_y) = \sum_{m=0}^{\infty} \sum_{n=0}^{\infty} \frac{(ik_x)^m (ik_y)^n k_{m,n}}{m!\, n!} \tag{5.24}$$

The Fourier transform of the entire distribution $\tilde{K}$ is related to $\tilde{k}$ by Eq. (5.2). We have evaluated $\tilde{K}$ numerically using these three equations; the square of $\tilde{K}$ is shown in Fig. 10, which approximates the diffraction pattern through a snowflake-shaped slit. From this figure it is evident that $\tilde{K}$ has the same symmetry group as the hexagon (D_6).

For the fractal distributions in previous sections, which did not have transformations involving rotations, showing that the Fourier transform did not approach zero as $|\mathbf{k}| \to \infty$ was trivial. In this case, the proof requires more work.

The transformations in Eq. (5.23) are given by a dilation of $1/\sqrt{3}$ and a rotation of an odd multuple of $\pi/6$. (The second transformation also involves a reflection which makes no difference here). Thus six points on the vertices of a hexagon are mapped to the vertices of a smaller hexagon,

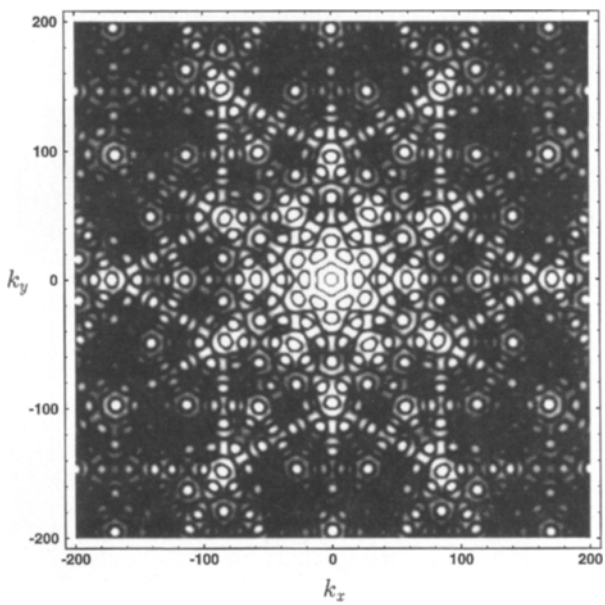

Fig. 10. The square of the Fourier transform of the von Koch snowflake. Lighter shades correspond to larger values, with white denoting all values above 0.007.

which is rotated by $\pi/6$. The value of $\tilde{k}$ at a single point far from the origin can thus be evaluated in terms of $\tilde{k}$ at only six points, which lie on the vertices of a hexagon, and a complicated combination of the exponentials in Eq. (5.23). It is not difficult to check that it depends on the values at all six of these points.

The values of $\mathbf{k}$ for which both exponentials in Eq. (5.23) are equal to 1 lie on a periodic lattice with basis vectors $(3\pi, \sqrt{3}\pi)$ and $(-3\pi, \sqrt{3}\pi)$. This lattice is invariant under $\pi/3$ rotations, and also the inverse of the transformations in Eq. (5.23), that is, $L_\alpha^{\dagger -1}$. Hence there exist arbitrarily large values of $|\mathbf{k}|$ for which all the transformations involve exponentials equal to 1, until the innermost hexagon of lattice points is reached. Where the exponentials are 1, $\tilde{k}$ is given as the arithmetic mean of two of its values at points in the inner hexagon. This means that, for one of the large values of $|\mathbf{k}|$ above, $\tilde{k}$ is approximately equal to the arithmetic mean of all six of its values at the inner hexagon. Numerically, this arithmetic mean is -0.066534. Thus $\tilde{k}$ does not tend to zero for large $|\mathbf{k}|$. Similarly, $\tilde{K}$ does not tend to zero either.

It is clear that the von Koch snowflake is a very special example; the translation vectors $\mathbf{t}_\alpha$ which generate the lattice of points must be consistent with the linear parts of the transformations which determine the points at which the Fourier transform is evaluated. It is clear that many self-similar fractals do not satisfy the stringent conditions required for the Fourier transform to contain peaks at large $|\mathbf{k}|$. There are, for example, no periodic lattices with fivefold symmetry, although this does not preclude the possibility of the exponentials in the recursion relation approaching 1 only in the large-$|\mathbf{k}|$ limit of the iterated transformations. For example, there are no periodic lattices invariant under a dilation factor of $\phi = (1+\sqrt{5})/2$, but multiple transformations yield ϕ^n, which is arbitrarily close to an integer for all n sufficiently large.

6. SUMMARY AND DISCUSSION

A number of general statements may be made concerning the analytic properties of functions derived from fractal distributions. The self-similarity of a charge distribution may be used, together with Mellin transform techniques, to find an expansion for the potential near a point in the distribution. The potential follows a power law in the distance from the distribution, together with small oscillatory terms and a Taylor series. The exponent is an effective dimension of the distribution: the Hausdorff dimension in the case of a uniform distribution, as in Eq. (5.13), or some other effective dimension of a multifractal distribution, as in Eq. (3.14).

A simple recursion relation for the moments may be derived. If the transformations defining the fractal do not contain rotations, the moments may be evaluated directly, otherwise simultaneous linear equations must be solved. The asymptotic behavior of the moments is closely related to that of the potential close to the distribution, and thus involves the effective dimension(s) of the distribution. This connection is difficult to exploit unless the fractal has embedding dimension $E=1$, as in Eq. (3.46). For more complicated cases, it appears that, in addition, E appears in the asymptotic behavior of the moments, Eq. (4.7), but is not the only determining factor, Eqs. (5.21), (5.22).

The Fourier transform of a self-similar distribution may be written an infinite product of sums of exponentials if the linear parts of all the transformations are equal, Eq. (2.15). This is a slight generalization of the result in ref. 7, although this paper includes some related, but not self-similar fractals, which we do not. For large values of $\mathbf{k}$ the Fourier transform may or may not tend to zero, depending on the transformations defining the distribution. A discussion of this point for the case without rotations is contained in ref. 7. From our analysis it appears that the von Koch snowflake is a rare example of a fractal defined using rotations for which the Fourier transform does not tend to zero for large $\mathbf{k}$. Averaging over $\mathbf{k}$, we find that the Fourier transform of the binomial Cantor distribution decreases at a rate related to its smallest effective dimension, Eq. (3.54). For the case of the Menger sponge this rate depended on other parameters, not directly related to the dimension, Eq. (4.15).

There is clearly much scope for further work. The full structure of the moments and Fourier transform of fractals with $E>1$ remains to be clarified.[17] There are also problems in the potential theory of fractals with different boundary conditions, such as fixing the potential on the fractal, and solving for the charge distribution. As argued by Evertz and Mandelbrot,[3] the charge distribution for this class of problem is multifractal, but it is not exactly self-similar.

ACKNOWLEDGMENTS

The authors wish to thank Dr. Michael Shlesinger and Dr. Vic Kowalenko for helpful discussions and A. Logothetis for assistance with the numerical computations. One of us (C.D.) acknowledges the support of an Australian Postgraduate Research Award.

REFERENCES

1. P. Carruthers, *Astrophys. J.* **380**:24 (1991).
2. J. E. Avron and B. Simon, *Phys. Rev. Lett.* **46**:1166 (1981).
3. C. J. G. Evertz and B. B. Mandelbrot, *J. Phys. A* **25**:1781 (1992).
4. B. Sapoval, T. Gobron, and A. Margolina, *Phys. Rev. Lett.* **67**:2974 (1991).
5. D. Berger, S. Chamaly, M. Perreau, D. Mercier, P. Monceau, and J.-C. S. Levy, *J. Phys. I* **1**:1433 (1991).
6. M. V. Berry, *J. Phys. A* **12**:781 (1979).
7. C. Allain and M. Cloitre, *Phys. Rev. A* **36**:5751 (1987).
8. C. Allain and M. Cloitre, *Physica A* **157**:352 (1989).
9. P. D'Antonio and J. Konnert, *J. Audio Eng. Soc.* **40**:117 (1992).
10. K. Falconer, *Fractal Geometry and Its Applications* (Wiley, Chichester, 1990).
11. N. S. Landkof, *Foundations of Modern Potential Theory* (Springer-Verlag, Berlin, 1972).
12. D. Bessis, J. S. Geronimo, and P. Moussa, *J. Stat. Phys.* **34**:75 (1984).
13. C. P. Dettmann and N. E. Frankel, *J. Phys. A* **26**:1009 (1993).
14. F. Hille and J. D. Tamarkin, *Am. Math. Monthly* **36**:255 (1929).
15. F. Oberhettinger, *Tables of Mellin Transforms* (Springer-Verlag, Berlin, 1974).
16. B. B. Mandelbrot, *The Fractal Geometry of Nature* (Freeman, New York, 1977).
17. C. P. Dettmann and N. E. Frankel, *Fractals* Vol. 1, No. 2, (1993), in press.